

# Basolateral Na<sup>+</sup>-dependent HCO<sub>3</sub><sup>-</sup> transporter NBCn1-mediated HCO<sub>3</sub><sup>-</sup> influx in rat medullary thick ascending limb

Elvin Odgaard<sup>1,2,§</sup>, Jakob K. Jakobsen<sup>1,2,§</sup>, Sebastian Frische<sup>2</sup>, Jeppe Praetorius<sup>2</sup>, Søren Nielsen<sup>2</sup>, Christian Aalkjær<sup>1,2</sup> and Jens Leipziger<sup>1,2</sup>

<sup>1</sup>Institute of Physiology and <sup>2</sup>The Water and Salt Research Center, University of Aarhus, Denmark

The electroneutral Na<sup>+</sup>-dependent HCO<sub>3</sub><sup>-</sup> transporter NBCn1 is strongly expressed in the basolateral membrane of rat medullary thick ascending limb cells (mTAL) and is up-regulated during NH<sub>4</sub><sup>+</sup>-induced metabolic acidosis. Here we used *in vitro* perfusion and BCECF video-imaging of mTAL tubules to investigate functional localization and regulation of Na<sup>+</sup>-dependent HCO<sub>3</sub><sup>-</sup> influx during NH<sub>4</sub><sup>+</sup>-induced metabolic acidosis. Tubule acidification was induced by removing luminal Na<sup>+</sup> ( $\Delta\text{pH}_i$ :  $0.88 \pm 0.11$  pH units,  $n = 10$ ). Subsequently the basolateral perfusion solution was changed to CO<sub>2</sub>/HCO<sub>3</sub><sup>-</sup> buffer with and without Na<sup>+</sup>. Basolateral Na<sup>+</sup>-H<sup>+</sup> exchange function was inhibited with amiloride. Na<sup>+</sup>-dependent HCO<sub>3</sub><sup>-</sup> influx was determined by calculating initial base flux of Na<sup>+</sup>-mediated re-alkalinization. In untreated animals base flux was  $8.4 \pm 0.9$  pmol min<sup>-1</sup> mm<sup>-1</sup>. A 2.4-fold increase of base flux to  $21.8 \pm 3.2$  pmol min<sup>-1</sup> mm<sup>-1</sup> was measured in NH<sub>4</sub><sup>+</sup>-treated animals (11 days,  $n = 11$ ). Na<sup>+</sup>-dependent re-alkalinization was significantly larger when compared to control animals ( $0.38 \pm 0.03$  versus  $0.22 \pm 0.02$  pH units,  $n = 10$ ). In addition, Na<sup>+</sup>-dependent HCO<sub>3</sub><sup>-</sup> influx was of similar magnitude in chloride-free medium and also up-regulated after NH<sub>4</sub><sup>+</sup> loading. Na<sup>+</sup>-dependent HCO<sub>3</sub><sup>-</sup> influx was not inhibited by 400  $\mu\text{M}$  DIDS. A strong up-regulation of NBCn1 staining was confirmed in immunolabelling experiments. RT-PCR analysis revealed no evidence for the Na<sup>+</sup>-dependent HCO<sub>3</sub><sup>-</sup> transporter NBC4 or the two Na<sup>+</sup>-dependent Cl<sup>-</sup>/HCO<sub>3</sub><sup>-</sup> exchangers NCBE and NDCBE. These data strongly indicate that rat mTAL tubules functionally express basolateral DIDS-insensitive NBCn1. Function and protein are strongly up-regulated during NH<sub>4</sub><sup>+</sup>-induced metabolic acidosis. We suggest that NBCn1-mediated basolateral HCO<sub>3</sub><sup>-</sup> influx is important for basolateral NH<sub>3</sub> exit and thus NH<sub>4</sub><sup>+</sup> excretion by means of setting pH<sub>i</sub> to a more alkaline value.

(Received 6 May 2003; accepted after revision 10 December 2003; first published online 12 December 2003)

Corresponding author J. Leipziger: Ole Worms Allé 160, 8000 Aarhus C, Denmark. Email: leip@fi.au.dk

The thick ascending limb of Henle's loop (TAL) serves a number of important transport functions. On the one hand it is critically involved in NaCl absorption, generation of high interstitial osmolality and thus the countercurrent system of urine concentration (Greger, 1985). In addition it is involved in the regulation of acid–base homeostasis. Up to 15% of HCO<sub>3</sub><sup>-</sup> is absorbed in TAL, all of which appears dependent on the presence of the luminal Na<sup>+</sup>-H<sup>+</sup> exchanger NHE3 (Good *et al.* 1984; Good, 1985). Subsequently mTAL is involved in the excretion of NH<sub>4</sub><sup>+</sup>. NH<sub>4</sub><sup>+</sup> entering the loop of Henle is

able to travel transcellularly and uses a 'medullary short cut' to eventually appear in the collecting duct (Good, 1994).

Recently an electroneutral Na<sup>+</sup>-dependent HCO<sub>3</sub><sup>-</sup> cotransporter (NBCn1) was cloned (Choi *et al.* 2000) and immunolabelling demonstrated its presence in basolateral membrane domains of thick ascending limb in rat kidney outer medulla (Vorum *et al.* 2000). The labelling was more pronounced in the inner stripe of the outer medulla (ISOM), somewhat less in the outer stripe of the outer medulla and absent in the cortex (Vorum *et al.* 2000). An electroneutral Na<sup>+</sup>-dependent HCO<sub>3</sub><sup>-</sup> transporter with a proposed stoichiometry of 1 Na<sup>+</sup> and 1 HCO<sub>3</sub><sup>-</sup> will function as a HCO<sub>3</sub><sup>-</sup> importer (Choi *et al.* 2000).

§These authors contributed equally to this work.

Indeed, basolateral  $\text{Na}^+$ -dependent  $\text{HCO}_3^-$  influx was identified recently in isolated perfused rat medullary thick ascending limbs (Bourgeois *et al.* 2002). Apparently, this is in conflict with the need for basolateral  $\text{HCO}_3^-$  extrusion during  $\text{HCO}_3^-$  absorption (Good *et al.* 1984; Good, 1985). As such, the functional significance of a basolateral  $\text{Na}^+$ -dependent  $\text{HCO}_3^-$  importer remains undefined. A subsequent study from our group identified that NBCn1 protein is strongly up-regulated in a rat model of chronic metabolic acidosis induced by either  $\text{NH}_4^+$  feeding or inclusion of  $\text{NH}_4^+$  into the drinking water (Kwon *et al.* 2002). Thus we have speculated that NBCn1 may play a significant role in the excretion of  $\text{NH}_4^+$  (Kwon *et al.* 2002).  $\text{NH}_4^+$  that has entered the mTAL cell via the furosemide (frusemide)-sensitive NKCC2 transporter or the ROMK channel will dissociate into  $\text{NH}_4^+$  and  $\text{NH}_3$ . The generated  $\text{NH}_3$  will leave the cell via non-ionic diffusion preferentially over the basolateral membrane and finally is transported into the acidic compartment of the collecting duct. The remaining proton may either be transported directly via a  $\text{Na}^+$ - $\text{H}^+$  antiporter and/or could be buffered by import of  $\text{HCO}_3^-$ . The generation of  $\text{CO}_2$  would subsequently allow for the recycling of  $\text{HCO}_3^-$  over the basolateral membrane. In this hypothesis the extrusion of a proton/import of a  $\text{HCO}_3^-$  ion serves to set  $\text{pH}_i$  to more alkaline values, a state where, for example,  $\text{NH}_3$  extrusion but also  $\text{NaCl}$  absorption is less restrained. Thus the purpose of this study was to functionally localize  $\text{Na}^+$ -dependent  $\text{HCO}_3^-$  uptake in the intact, isolated perfused mTAL tubules. Furthermore it was intended to investigate if basolateral  $\text{Na}^+$ -dependent  $\text{HCO}_3^-$  uptake is functionally up-regulated in rats treated with added  $\text{NH}_4^+$  in their drinking water, a well-known condition for up-regulated NBCn1 expression (Kwon *et al.* 2002).

## Methods

### Tubule perfusion

All handling and use of the animals complied with Danish animal welfare regulations. Experiments were carried out using 4- to 6-week-old female Wistar rats weighing 70–80 g. The animals were divided into two age-matched groups. The control group had free access to food (standard rat laboratory diet, Altromin, Lage, Germany) and tap water. Also in the experimental group the animals had free access to food and water. Their drinking water contained 0.196 M ammonium chloride as previously described (Kwon *et al.* 2002). Animals were killed after  $8.0 \pm 1.4$  days ( $n = 11$ ) by decapitation, and the left or right kidney was removed rapidly, placed in ice-cold

Ringer solution (see below) and subsequently sliced as previously described (Wright *et al.* 1990). Kidney slices were transferred into a dissection chamber continuously cooled at 4°C and gassed with carbogen (5%  $\text{CO}_2$ –95%  $\text{O}_2$ ). Medullary thick ascending limbs (mTAL) were dissected from the inner stripe of the outer medulla using ultrafine watchmaker forceps. The kidney tubules were transferred into a specialized perfusion chamber mounted on an inverted microscope. Isolated tubules were perfused using a system of concentric glass pipettes previously used and developed by R. F. Greger and W. Hampel (Greger & Hampel, 1981).

### Digital video imaging

The set-up consisted of an inverted microscope (Axiovert 100 TV, Zeiss, Jena, Germany) with a  $\times 63$  objective (C-Apochromat  $\times 63$ , 1.2 water, Zeiss, Jena, Germany), a monochromator (Polychrome IV, Till Photonics, Planegg, Germany) and a digital camera (MicroMax, 5 MHz, Princeton Instruments, NJ, USA). Image acquisition and data analysis were performed with the software package Metamorph/Metafluor (Universal Imaging, West Chester, PA, USA). Freshly dissected mTAL were mounted into the perfusion system (Greger & Hampel, 1981). Measurement of  $\text{pH}_i$  was performed with the 2',7'-bis-(2-carboxyethyl)-5-(and-6)-carboxyfluorescein (BCECF). Tubules were incubated in 20  $\mu\text{M}$  basolateral BCECF/AM for 20 min at room temperature in control solution (No. 1, see Table 1). As a measure of  $\text{pH}_i$  the fluorescence emission ratio at 488 nm/436 nm excitation was used and the recording speed was 1–2 Hz. Care was taken to reduce cellular damage induced by excitation light (Weiner & Hamm, 1989). This was accomplished by using neutral grey filters in the excitation light path and a 4-fold binning function of the imaging system. In each experiment the fluorescence signal was recorded from the entire tubule. The average length of the perfused tubule was around 300  $\mu\text{m}$ . During the dye-loading period the tubule was continuously perfused from the luminal side with solution 1. The experiment was started 5–10 min after washout of extracellular dye and after a stable fluorescence ratio was reached. Depending on the viability of the individual tubule, stable BCECF 488 nm/436 nm ratios could be measured for 45 min or more.

BCECF signals were calibrated using the high  $\text{K}^+$ -nigericin method at the end of the experiment (Thomas *et al.* 1979). The following calibration solution previously used by others for the same tubule segment (Watts *et al.* 1994) was used and contained (mM): KCl 95,  $\text{NaH}_2\text{PO}_4$  0.4,  $\text{Na}_2\text{HPO}_4$  1.6, glucose 5,  $\text{MgCl}_2$  1, calcium gluconate 1.3, Hepes 25, *N*-methyl-D-glucamine (NMDG) 20 and NaCl 15.

**Table 1. Experimental solutions**

Component	No. 1: Hepes	No. 2: Hepes	No. 3: HCO <sub>3</sub> <sup>-</sup>	No. 4: HCO <sub>3</sub> <sup>-</sup>	No. 5: HCO <sub>3</sub> <sup>-</sup>	No. 6: HCO <sub>3</sub> <sup>-</sup>	No. 7: Hepes
	HCO <sub>3</sub> <sup>-</sup> free	Na <sup>+</sup> free HCO <sub>3</sub> <sup>-</sup> free		Na <sup>+</sup> free	Cl <sup>-</sup> free	Cl <sup>-</sup> free, Na <sup>+</sup> free	Cl <sup>-</sup> free, Na <sup>+</sup> free
NaCl	145	—	118	—	—	—	—
NMDG	—	145	—	120	—	119	145
KH <sub>2</sub> PO <sub>4</sub>	0.4	0.4	0.4	0.4	0.4	0.23	0.4
K <sub>2</sub> HPO <sub>4</sub>	1.6	1.6	1.6	1.6	1.6	0.95	1.6
Glucose	5	5	5	5	5	5	5
Hepes	5	5	5	5	5	5	5
MgCl <sub>2</sub>	1	1	1	1	—	—	—
MgSO <sub>4</sub>	—	—	—	—	—	6	—
Ca gluconate	1.3	1.3	1.3	1.3	8	4	4
EDTA	—	—	—	—	—	0.026	—
NaHCO <sub>3</sub> <sup>-</sup>	—	—	24	—	24	—	—
HCl	—	130	—	100	—	—	—
Choline-HCO <sub>3</sub> <sup>-</sup>	—	—	—	24	—	24	—
Na gluconate	—	—	—	—	121	—	—
Gluconic acid	—	—	—	—	—	121	145

All solutions had a pH of 7.40 prior to experiments. All solutions were gassed with carbogen (5% CO<sub>2</sub>–95% O<sub>2</sub>) except for solutions 1 and 7.

### Measurement of intracellular buffering capacity

Quantification of HCO<sub>3</sub><sup>-</sup> transport requires the knowledge of intracellular buffering capacity  $\beta_i$ . We therefore measured the intracellular buffering capacity in normal and NH<sub>4</sub><sup>+</sup>-treated animals using a similar protocol to that described by D. Good (Watts *et al.* 1994). To minimize the effect of HCO<sub>3</sub><sup>-</sup>/CO<sub>2</sub> buffering and to block Na<sup>+</sup>-dependent pH<sub>i</sub> regulatory mechanisms Na<sup>+</sup>-free Hepes-containing solution (No. 1) was used on both sides of the tubule. In addition 5 mM Ba<sup>2+</sup>, 100  $\mu$ M furosemide and 1 mM ouabain were added to the bath. Subsequent addition of 2.5 mM trimethylamine to the bath rapidly increased mTAL pH<sub>i</sub> by  $0.26 \pm 0.03$  units in normal and  $0.19 \pm 0.02$  units in NH<sub>4</sub><sup>+</sup>-treated rats.  $\beta_i$  was calculated as  $\Delta[\text{HB}^+]/\Delta\text{pH}_i$ , where  $\Delta\text{pH}_i$  is the increase in pH<sub>i</sub> resulting from weak base addition and  $\Delta[\text{HB}^+]$  is the change in intracellular trimethylammonium concentration, calculated from its pK<sub>a</sub> (9.8 at 37°C) and assuming that the concentration of trimethylamine base is equal in intracellular and extracellular fluids at steady state. pH<sub>i</sub> values in the experiments for measuring  $\beta_i$  corresponded closely to pH<sub>i</sub> values in the experiments in which Na<sup>+</sup>-dependent HCO<sub>3</sub><sup>-</sup> influx was quantified (pH<sub>i</sub> 6.4). In normal rat tubules  $\beta_i$  was calculated to be  $98 \pm 16$  mM ( $n = 5$ ), which was not significantly different from  $114 \pm 12$  mM ( $n = 8$ ) found in tubules from NH<sub>4</sub><sup>+</sup>-treated animals.

### Calculation of base flux

Base flux ( $J_{\text{base}}$ ) (in pmol min<sup>-1</sup> mm<sup>-1</sup>) was calculated using the following equation:  $J_{\text{base}} = \Delta\text{pH}_i/\Delta t \times \beta_{\text{total}} \times$

$V$ , where  $\Delta\text{pH}_i/\Delta t$  is the initial rate of pH<sub>i</sub> change (in pH units min<sup>-1</sup>),  $\beta_{\text{total}}$  is the total cellular buffering capacity (in mM (pH unit)<sup>-1</sup> l<sup>-1</sup>), and  $V$  is the cell volume (in nl) per 1 mm of tubule length. pH<sub>i</sub> changes were determined by a linear fit of the pH<sub>i</sub> rise during the first 10–20 s after re-addition of Na<sup>+</sup>. To account for the increased buffering capacity in CO<sub>2</sub>/HCO<sub>3</sub><sup>-</sup>-containing solutions  $\beta_{\text{total}}$  was calculated as  $\beta_i + 2.3 \times [\text{HCO}_3^-]_i$ , where  $[\text{HCO}_3^-]_i$  is the intracellular HCO<sub>3</sub><sup>-</sup> concentration (Roos & Boron, 1981).  $[\text{HCO}_3^-]_i$  was calculated as follows:  $[\text{HCO}_3^-]_i = 0.03 P_{\text{CO}_2} \times 10^{(\text{pH}_i - 6.1)}$ . In carbogen-gassed solutions,  $P_{\text{CO}_2}$  was assumed to be 37 mmHg.  $V$  (0.32 nl mm<sup>-1</sup>) was calculated by measuring the dimensions of the tubule (volume = (radius of the tubule)<sup>2</sup>  $\times$   $\pi$   $\times$  length) with subtraction of the volume of the tubule lumen. A positive ( $J_{\text{base}}$ ) value indicates a net base influx.

### Solutions and chemicals

All experimental solutions not mentioned directly in the text are listed in Table 1. BCECF was obtained from Molecular Probes (Eugene, OR, USA). All other chemicals were of the highest grade of purity available and were obtained from Sigma-Aldrich Denmark (Vallensbæk Strand) and Merck (Darmstadt, Germany).

### Immunohistochemistry

Kidneys from six NH<sub>4</sub>Cl-loaded rats and six control rats were fixed by retrograde perfusion via the aorta with 4% paraformaldehyde in 0.1 M cacodylate buffer (pH 7.4)

**Table 2. Primers used to identify NBCn1, NBC4, NCBE, NDCBE, NKCC2 and BTR1 transcripts**

Transporter		Primer (5'–3')	Gene accession number
NBCn1*	F	GACTCCATAAGGGAGAATGTTCTGA	AF080106 (rat)
A-cassette	R	TCACCACTTTTACTACTGTCCAGG	
NBCn1**	F	CAAGCTCATGGATCTGTGC	AF080106 (rat)
B-cassette	R	ACTCACAGGCTTTTCAGGG	
NBC4	F	ATGGAGAGCTTCTGGGCAC	AF243499 (human)
	R	CTCAGCAGAGACCACTCCAG	
NCBE	F	GCAGGTCAGGTTGTTTCTCTCTC	NM_022058 (human)
	R	TCTTCTCTTCTCTGGGAAGG	
NDCBE	F	GCTCAAGAAAGGCTGTGGCTAC	NM_004858 (human)
	R	ACGCCTAATGACCCAGAGCAG	
BTR1	F	CACCTGCTGTGAGATACCATCC	AF336127 (human)
	R	TGGTGAGCAGCTGTCTCTGATG	
NKCC2	F	CAGTGGTGCCAGTCGTTTCC	NM_019134 (rat)
	R	TGGTGTGTGGCCAAAGGTT	

\*These primers were designed to be able to recognize if NBCn1 transcripts contain exon 7 (with 369 bp) and the so-called 'A-cassette' (42 bp) (Choi *et al.* 2000). \*\*These primers were designed to be able to recognize if NBCn1 transcripts contain the so-called 'B-cassette' (108 bp) (Choi *et al.* 2000). F, forward; R, reverse primers.

and postfixed for 30 min in the same fixative. Kidney slices containing all kidney zones were dehydrated and embedded in paraffin. The paraffin embedded tissues were cut at 2  $\mu$ m on a rotary microtome (Leica, Germany). The sections were dewaxed in xylene followed by rehydration to 99% and 96% ethanol. At this point, the sections were incubated in 0.3% H<sub>2</sub>O<sub>2</sub> in methanol to block endogenous peroxidase activity. After a rinse in 96% ethanol, the sections were rehydrated using 70% ethanol and finally water. To reveal antigens, sections were placed in 1 mM Tris buffer (pH 9.0) supplemented with 0.5 mM EGTA (3,6-di-oxa-octa-methylene-di-nitrilo-tetra-acetic acid) and heated in a microwave oven for 10 min. Non-specific binding of immunoglobulin was prevented by incubating the sections in 50 mM NH<sub>4</sub>Cl for 30 min followed by blocking in PBS supplemented with 1% BSA, 0.05% saponin and 0.2% gelatine. Sections were incubated overnight at 4°C with NBCn1 antibodies diluted in 10 mM PBS (pH 7.4) containing 0.1% Triton X-100 and 0.1% BSA. Subsequently, the sections were incubated with horseradish peroxidase-linked goat anti-rabbit secondary antibodies (P448, DAKO Glostrup, Denmark). The labelling was visualized by the diaminobenzidine (DAB) technique and the sections counterstained using Mayer's haematoxylin.

The previously described antibodies against NBCn1 (Vorum *et al.* 2000) and NBCe1 (anti-rkNBC1-CT15) (Maunsbach *et al.* 2000) were used in this study.

#### RT-PCR from microdissected mTAL segments

Using a commercially available kit (Trizol reagent, Invitrogen Life Technology, USA) total RNA was isolated

from 10 microdissected mTAL segments (approx. 2 mm of renal tubule). Isolated total RNA was transcribed into cDNA using the RETROscript Kit (Ambion, TX, USA). The primers shown in Table 2, derived from cloned rat or human sequences, were used to identify NBCn1, NBC4, NCBE, NDCBE, NKCC2 and BTR1 transcripts. Primers derived from human cDNA were aligned with the corresponding rat genomic sequences (<http://www.ensembl.org>). Thus the human and rat sequences were identical for the chosen regions of interest.

#### Statistics

The data shown are either original traces or mean values  $\pm$  s.e.m. (*n*), where *n* refers to the number of experiments. Paired or unpaired *t* tests were used to compare mean values within or between experimental series. A *P* value of <0.05 was taken to indicate statistical significance.

#### Results

##### Immunolabelling of NBCn1 in normal and NH<sub>4</sub><sup>+</sup>-treated young rats

The preceding study identified a strong up-regulation of NBCn1 protein in 'older' rats (mean body weight 250 g) treated with NH<sub>4</sub><sup>+</sup> (Kwon *et al.* 2002). Since successful microdissection of intact single isolated mTAL tubules is critically dependent on the age of the animal, it was necessary to choose significantly younger rats for this study. Tubule dissection in young rats weighing between 70 and 80 g renders sufficient access to single nephron segments, whereas this it is profoundly more

difficult in older animals. We thus repeated the initial immunolabelling experiments in young rats (weighing 70–80 g). Labelling of NBCn1 was compared in untreated and treated young rats (70–80 g). Treated rats received NH<sub>4</sub><sup>+</sup> in their drinking water for 8 days (see Methods). The previously measured NH<sub>4</sub><sup>+</sup>-induced metabolic acidosis (Kwon *et al.* 2002) was confirmed by measuring urine pH which was 7.04 ± 0.18 units in normal and 5.9 ± 0.08 units in NH<sub>4</sub><sup>+</sup>-treated animals (*n* = 6). As apparent from Fig. 1 there was a very strong up-regulation of NBCn1 labelling in the inner stripe of the outer medulla (ISOM) confirming the observation in adult rats (Kwon *et al.* 2002).

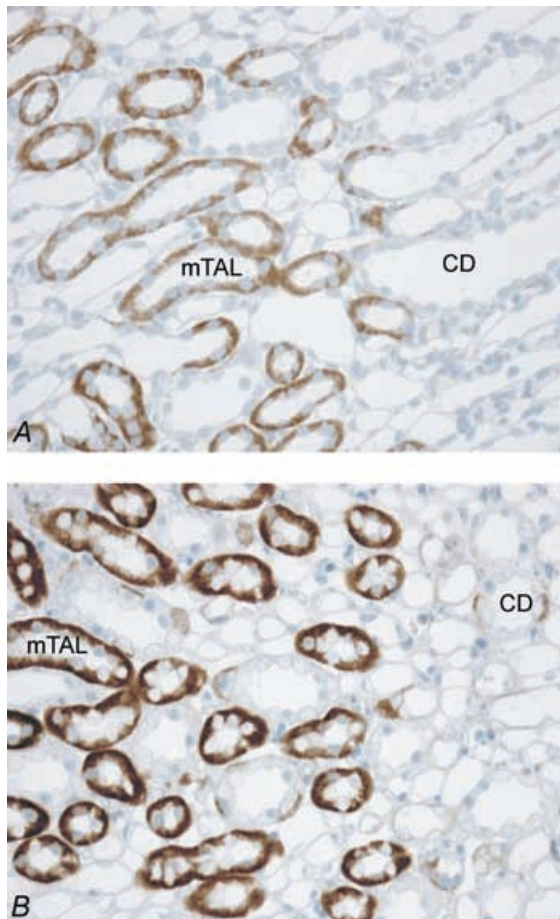


**Figure 1. Immunohistochemical localization of the electroneutral Na<sup>+</sup>-dependent HCO<sub>3</sub><sup>-</sup> transporter NBCn1 in control and NH<sub>4</sub>Cl-loaded rats**

NBCn1 was localized to the basolateral plasma membrane domains of mTAL segments in the inner stripe of the outer medulla and to the basolateral membrane of intercalated type A cells in collecting ducts. In comparison to controls (*A*), NH<sub>4</sub>Cl-loaded rats (*B*) showed a marked increase of NBCn1 labelling. mTAL, medullary thick ascending limb; CD, collecting duct.

**RT-PCR analysis**

NBCn1 as isolated from a smooth muscle library was shown to represent three different variants (NBCn1B, C or D) (Choi *et al.* 2000). The longest variant, NBCn1D, is composed of 1254 amino acid (AA) residues (3762 bp) (Fig. 2*D*). The two shorter variants lack either a so-called ‘A-cassette’ (14 AAs, NBCn1C) or the ‘B-cassette’ (36 AAs, NBCn1B). Close similarity was found to a human clone isolated from skeletal muscle. The authors assigned the name NBC3 to this isoform (Pushkin *et al.* 1999) (accession

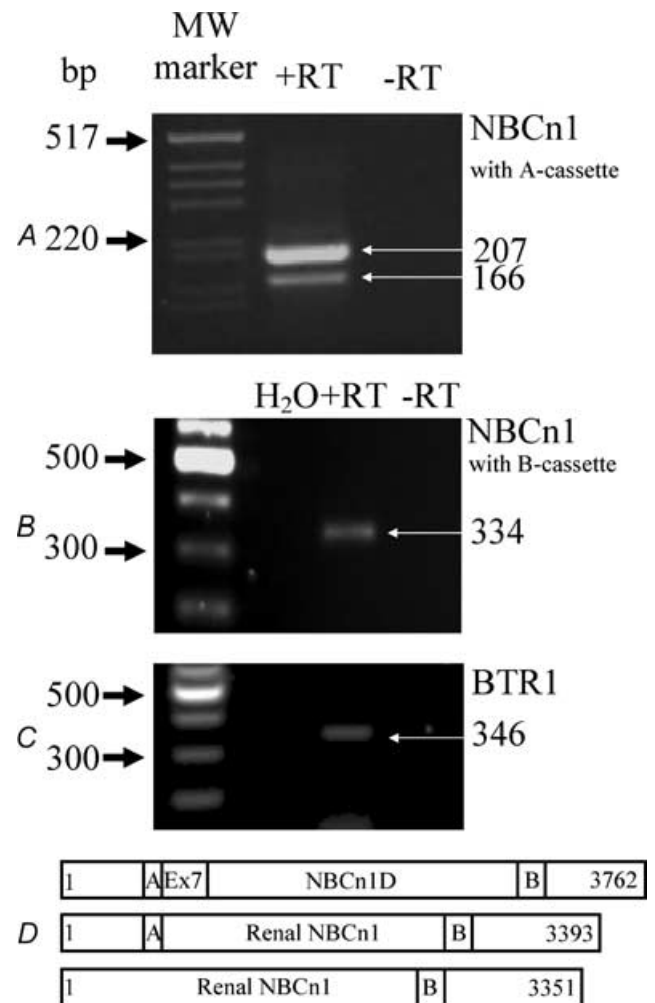


**Figure 2. RT-PCR characterization of NBCn1 message extracted from 10 single mTAL tubule segments**

Two different primer sets were used (Table 2) to investigate which splice variant is expressed in rat mTAL. The longer transcript in *A* (207 bp) reflects a message which does not contain the information of exon 7 but that of the so-called ‘A-cassette’. The shorter amplicon in *A* does not contain the A-cassette. The second primer set (*B*, Table 2) identified the presence of the so-called ‘B-cassette’ in renal NBCn1. In *D* the full length NBCn1 and the two different renal splice variants are depicted schematically. Also seen in Fig. 3*C* are data showing the specific message for BTR1 in single isolated mTAL tubules.

no. NM-003615). In a subsequent publication, the same group also identified a human kidney isoform of skeletal NBC3 termed NBC2b (accession no. AF089726). This isoform is lacking a segment of 369 bp corresponding to the information encoded in exon 7. Similar results (Fig. 2A) are presented here for the rat transcript of NBCn1. One set of primers was designed to recognize if the expected transcript contains exon 7 (bp 964–1332 in NBC1nD, gene accession number AF080106) and the 'A-cassette'. Our amplified cDNA from isolated mTAL tubules was near to 207 bp in size, as expected for a message without exon 7 but containing the 'A-cassette'. RT-PCR results with the same primers from heart or smooth muscle revealed a band size of close to 576 bp, indicating the expression of an exon 7-containing NBCn1 variant in those tissues (data not shown). Interestingly, an additional band of smaller size, close to 160 bp, was also amplified from the mTAL tubules. This is consistent with our interpretation that renal tubules also express a splice variant which does not contain the

'A-cassette'. The expected size of the amplified message without the 'A-cassette' is 166 bp. This and all the other reported PCR products generated with the different sets of primers were sequenced and identity with NBCn1 or other transporter messages confirmed. A second set of primers was designed to investigate if the mTAL NBCn1 contains the so-called 'B-cassette' (Table 2). As shown in Fig. 2B we found a single band of 334 bp indicating the presence of the 'B-cassette'. In summary, our single mTAL tubule RT-PCR approach identified that the predominant variant contains the 'A-' and the 'B-cassette' (Fig. 2D). Furthermore, an RT-PCR approach using single isolated mTAL tubules was used to investigate if specific mRNA transcripts for other known Na<sup>+</sup>-dependent HCO<sub>3</sub><sup>-</sup> transporters were expressed in rat mTAL. As quality control, single tubules were tested in parallel for the presence of NKCC2. Two independent tubule isolation procedures showed identical results. No evidence was found for the expression of NBC4, NCBE or NDCBE in isolated mTAL segments (see Fig. 3A–C) (See different primers and gene accession nos in Table 2.) Positive control RT-PCR amplicons for NBC4 were found in choroid plexus (502 bp), for NCBE in cerebellum (498 bp) and for NDCBE in cerebellum (472 bp) (Fig. 3A–C). Clear results were obtained for the expression of the

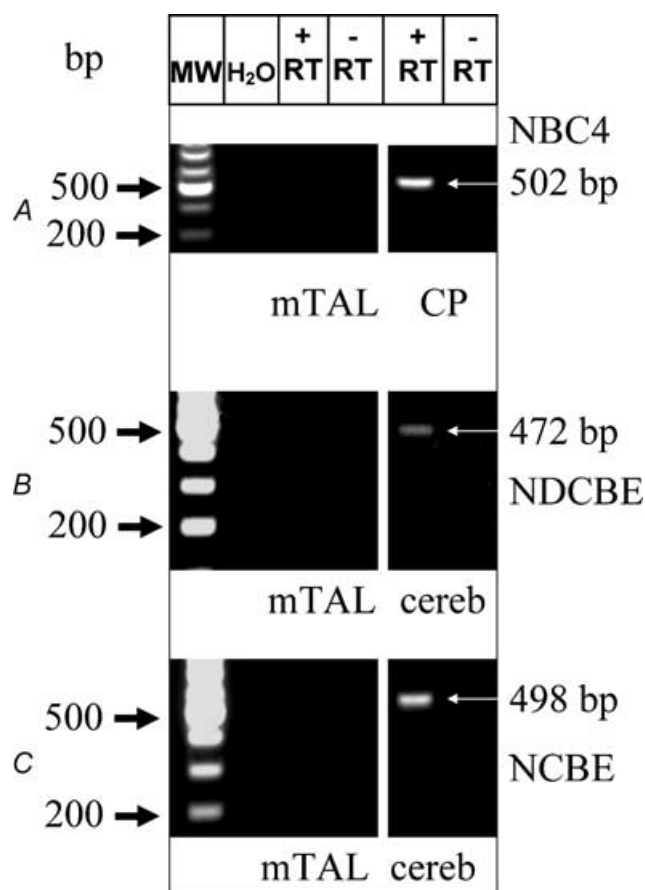


**Figure 3.** RT-PCR analysis of specific message for NBC4 (A), NDCBE (B) and NCBE (C) from 10 single mTAL tubule segments. No evidence was found for the expression of any of the three cotransporters. Positive controls for NBC4 were obtained from liver and for NDCBE and NCBE from cerebellum.

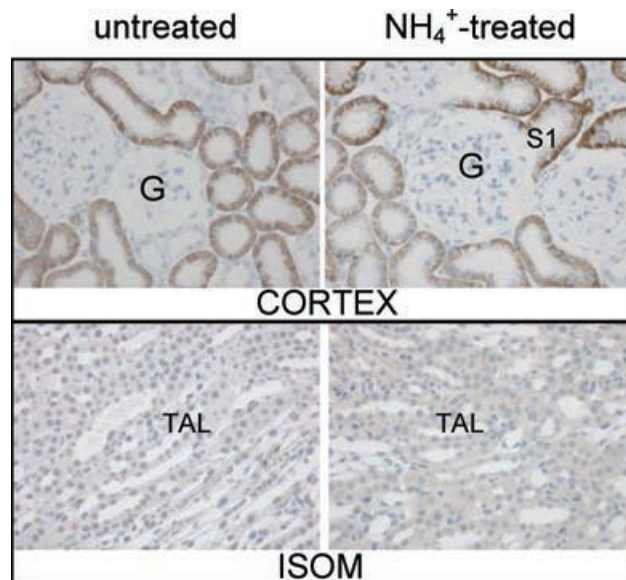


**Figure 4.** Immunohistochemical localization of NBCe1 in control and NH<sub>4</sub>Cl-loaded rats

NBCe1 was localized to the basolateral plasma membrane domains of proximal tubules in the renal cortex (upper panel). No up-regulation of NBCe1 staining was observed in NH<sub>4</sub>Cl-loaded rats. No immunolabelling of NBCe1 was seen in the same rats in the thick ascending limb in the inner stripe of the outer medulla (ISOM) or other nephron segments (lower panel). TAL, medullary thick ascending limb; G, glomerulus; S1, first segment of proximal tubule.

as yet uncharacterized BTR1 in isolated mTAL tubules, a novel member of the SLC4A solute carrier gene family (Fig. 2C). Despite the fact that the electrogenic  $\text{Na}^+$ -dependent  $\text{HCO}_3^-$  transporter (NBCe1) is known to be expressed only in kidney cortex (Maunsbach *et al.* 2000), we used immunohistochemistry to investigate if NBCe1 could be expressed in rat mTAL during  $\text{NH}_4^+$ -induced metabolic acidosis. The results are shown in Fig. 4. It can be clearly seen that NBCe1 is exclusively expressed in the proximal tubule and that no up-regulation occurs during metabolic acidosis. No NBCe1 labelling was observed in the inner stripe of outer medulla.

Thus our results strongly indicate that other members of the family of  $\text{Na}^+$ -coupled  $\text{HCO}_3^-$  transporters are not expressed in mTAL.

Subsequently we set out to investigate basolateral  $\text{Na}^+$ -dependent  $\text{HCO}_3^-$  import in  $\text{pH}_i$  measurements of isolated perfused mTAL segments.

### Calibration of $\text{pH}_i$

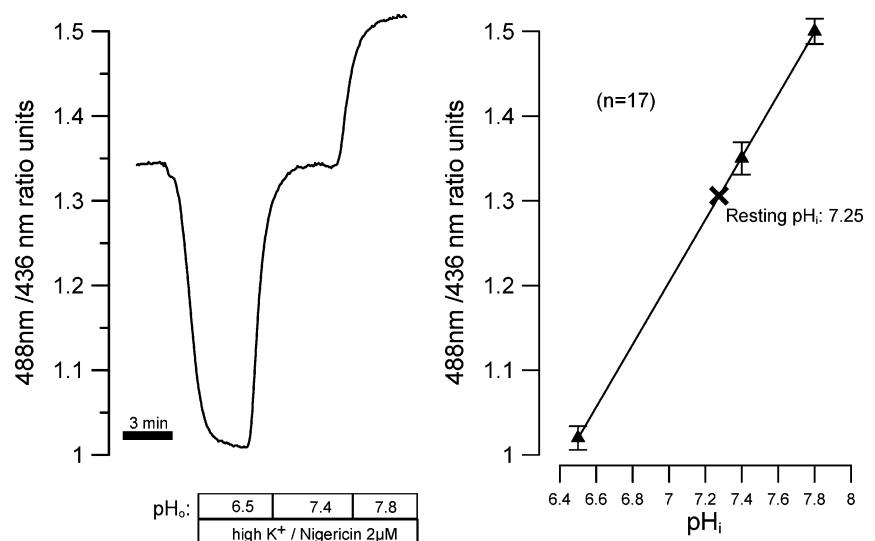
An original trace of a single calibration experiment is shown in Fig. 5. The right panel depicts the cumulative curve of 17 experiments. Calibrations were performed at the end of the experiments. In Hepes-buffered solution (No. 1) the resting  $\text{pH}_i$  was  $7.25 \pm 0.04$  units. In  $\text{HCO}_3^-/\text{CO}_2$ -containing buffer (solution No. 3) the resting  $\text{pH}_i$  was  $7.1 \pm 0.03$  units ( $n = 9$ ). No difference in resting  $\text{pH}_i$  was measured between normal and treated animals in the absence or presence of  $\text{HCO}_3^-$ .

### $\text{Na}^+$ -dependent recovery from acid load in $\text{HCO}_3^-$ -containing buffer

To evaluate NBCn1 function we measured basolateral  $\text{Na}^+$ -dependent import of  $\text{HCO}_3^-$  in isolated perfused mTAL segments. The following protocol as depicted in Fig. 6 was applied. It is well established in this nephron segment that removal of luminal  $\text{Na}^+$  induces a large intracellular acidification (Sun *et al.* 1992; Watts *et al.* 1994). This  $\text{pH}_i$  acidification reflects largely the activity of luminal  $\text{Na}^+-\text{H}^+$  (NHE3) exchange activity (Good & Watts, 1996). We therefore chose to acid-load mTAL segments by removing luminal  $\text{Na}^+$ . This also served the important purpose of excluding any effect of luminal NHE3 action when analysing  $\text{Na}^+$ -dependent recovery from acid load. As shown, removal of luminal  $\text{Na}^+$  strongly acidified  $\text{pH}_i$  by  $0.88 \pm 0.11$  units ( $n = 10$ ). In  $\text{NH}_4^+$ -treated animals this  $\text{pH}_i$  decrease amounted to  $0.64 \pm 0.08$  units ( $n = 11$ ). Subsequently the perfusion solution on the basolateral side was changed to solution No. 4 (see Table 1) containing  $\text{CO}_2/\text{HCO}_3^-$  and amiloride ( $300 \mu\text{M}$ ) but no  $\text{Na}^+$ . This led to a further stable acidification by  $0.16 \pm 0.05$  pH units in control rats ( $n = 10$ ) and  $0.42 \pm 0.07$  pH units in  $\text{NH}_4^+$ -treated rats ( $n = 11$ ). After 3 min, basolateral  $\text{Na}^+$  was added in the continuous presence of basolateral amiloride ( $300$  or  $600 \mu\text{M}$ ). Amiloride was used to minimize any effect of the basolateral NHE antiporter-mediated  $\text{H}^+$  efflux.  $\text{Na}^+$  addition in the presence of amiloride led to an instantaneous increase of  $\text{pH}_i$ . To establish the requirement for  $\text{HCO}_3^-$  in this re-alkalinization, the same experimental protocol was used

**Figure 5.  $\text{pH}_i$  calibration of BCECF signal in isolated mTAL segments using the high  $\text{K}^+$ -nigericin method**

Left panel, original BCECF fluorescence recording. Right panel, summary of 17 calibration experiments; resting  $\text{pH}_i$  of normal rats in Hepes buffer was 7.25



in  $\text{HCO}_3^-$ -free Hepes-buffered solution (solution No. 1). An original experiment is shown in Fig. 7. The addition of  $\text{Na}^+$  in the presence of  $300 \mu\text{M}$  basolateral amiloride induced a very small re-alkalinization ( $0.017 \pm 0.01$  pH units  $\text{min}^{-1}$ ,  $n = 6$ ). In another series of experiments we tested  $600 \mu\text{M}$  basolateral amiloride. Without amiloride the re-alkalinization was  $0.26 \pm 0.05$  pH units  $\text{min}^{-1}$  and was nearly completely (94.2%) inhibited to  $0.015 \pm 0.14$  pH units  $\text{min}^{-1}$  ( $n = 6$ ). Thus no apparent difference was

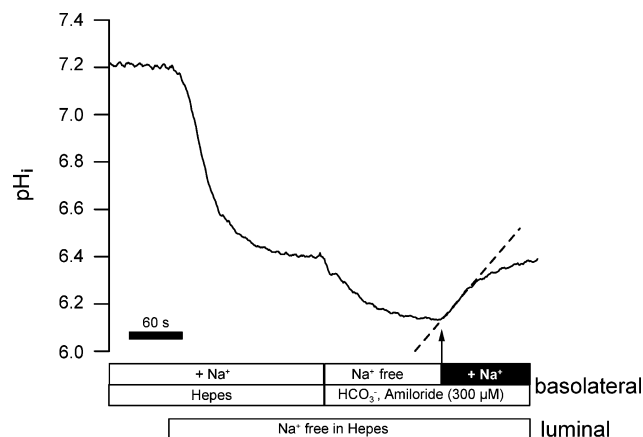


**Figure 6. Original experiment showing the protocol used to acidify mTAL segments**

See main text for detailed description. mTAL tubules were acidified by removal of luminal  $\text{Na}^+$ . Shifting basolateral Hepes buffer to  $\text{CO}_2/\text{HCO}_3^-$  buffer in the absence of basolateral  $\text{Na}^+$  mediated a further acidification. In the presence of basolateral amiloride re-addition of basolateral  $\text{Na}^+$  induced a rapid re-alkalinization. The dashed line indicates the initial rate of re-alkalinization.

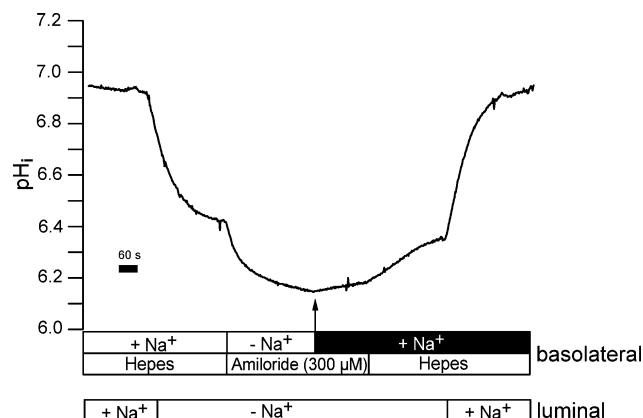


**Figure 7. Absence of basolateral  $\text{Na}^+$ -dependent re-alkalinization in Hepes buffer**

Original experiment of the same type as in Fig. 4 but in  $\text{HCO}_3^-$ -free Hepes-containing solution. mTAL tubules were acidified by removal of luminal  $\text{Na}^+$ . Removal of basolateral  $\text{Na}^+$  and addition of amiloride ( $300 \mu\text{M}$ ) induced a further acidification. In the presence of basolateral amiloride, re-addition of basolateral  $\text{Na}^+$  induced no significant re-alkalinization.

observed when using either  $300$  or  $600 \mu\text{M}$  amiloride. To minimize any eventual effects of the luminal acid–base transport molecules (NHE3 and  $\text{H}^+$ -ATPase), these experiments were conducted in the absence of luminal  $\text{Na}^+$  and in the presence of luminal amiloride ( $1 \text{ mM}$ ) and omeprazole ( $100 \mu\text{M}$ ). Therefore the large recovery from acid load shown in Fig. 6 has an absolute requirement for  $\text{HCO}_3^-$  and thus reflects basolateral  $\text{Na}^+$ -dependent import of  $\text{HCO}_3^-$ . The recovery rate from acid load was calculated from the initial (linear) increase of  $\text{pH}_i$ . The data of the first 10–20 s were fitted to a linear function and expressed  $\text{pH}_i$  change/time. Subsequently we investigated if  $\text{Na}^+$ -dependent  $\text{HCO}_3^-$  influx is also functional at less acidic  $\text{pH}_i$  values. To impose a less dramatic acidification, two different protocols were applied and are shown in Fig. 8. After changing from a Hepes-containing buffer to a  $\text{Na}^+$ -free solution containing  $\text{CO}_2/\text{HCO}_3^-$  with  $600 \mu\text{M}$  amiloride, the mTALs acidified from  $7.41 \pm 0.02$  to  $7.08 \pm 0.11$  pH units. Subsequent addition of basolateral  $\text{Na}^+$  induced a rapid alkalinization ( $0.26 \pm 0.07$  pH units  $\text{min}^{-1}$ ,  $n = 9$ ). Subsequently luminal NHE3 was inhibited with amiloride ( $1 \text{ mM}$ ). In basolateral  $\text{Na}^+$ -free solution this led to a further acidification to  $6.8 \pm 0.02$  units. The addition of  $\text{Na}^+$  under these conditions again induced a rapid re-alkalinization ( $0.32 \pm 0.13$  pH units  $\text{min}^{-1}$ ,  $n = 4$ ). Therefore,  $\text{Na}^+$ -dependent  $\text{HCO}_3^-$  influx is functional at all tested  $\text{pH}_i$  values ( $\text{pH}_i$  6.49, 6.80 and 7.08).

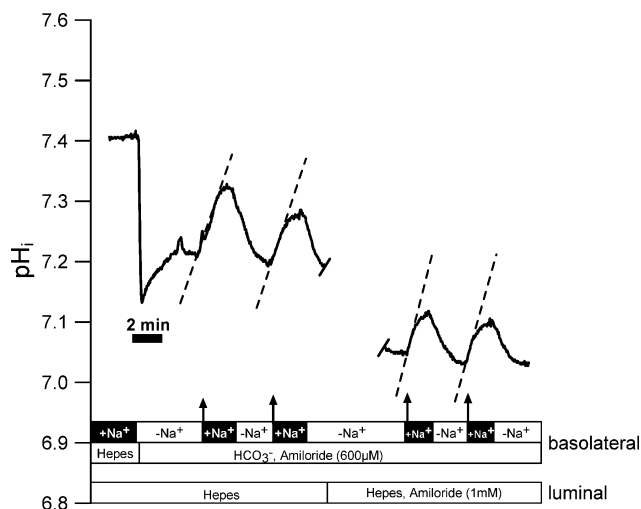


**Figure 8.  $\text{Na}^+$ -dependent  $\text{HCO}_3^-$  influx is present at different  $\text{pH}_i$  values**

mTAL tubules were acidified by luminal amiloride ( $1 \text{ mM}$ ) or in addition further acidified by basolateral amiloride ( $600 \mu\text{M}$ ). This original trace shows a decrease of  $\text{pH}_i$  to  $7.2$  or  $7.05$ , respectively. In both parts of the experiment addition of basolateral  $\text{Na}^+$  induced a rapid and reversible re-alkalinization.



**Up-regulation of Na<sup>+</sup>-dependent HCO<sub>3</sub><sup>-</sup> influx in NH<sub>4</sub><sup>+</sup>-treated animals**

Initially we tested whether Na<sup>+</sup>-H<sup>+</sup> exchange activity was altered in control *versus* NH<sub>4</sub><sup>+</sup>-treated rats. Interestingly no difference was observed. In control rats the Na<sup>+</sup>-dependent pHi recovery rate in Hepes-buffered solutions was 0.26 ± 0.05 *versus* 0.27 ± 0.04 pH units min<sup>-1</sup> in rats treated for 7.4 ± 0.7 days with NH<sub>4</sub><sup>+</sup> (n = 9). These results are supported by immunolabelling results showing no change of expression of the NHE1 protein in the basolateral membrane of normal *versus* NH<sub>4</sub><sup>+</sup>-treated animals (data not shown, S. Frische). The most important purpose of this study was to investigate if up-regulation of NBCn1 protein, seen in immunolabelling experiments and Western blotting (Kwon *et al.* 2002), correlates with an increase of basolateral Na<sup>+</sup>-dependent HCO<sub>3</sub><sup>-</sup> influx. Two single experiments in NH<sub>4</sub><sup>+</sup>-treated and untreated animals are depicted for comparison in Fig. 9. Isolated tubules were acidified as described and shown in Fig. 6. Two significant differences between normal and NH<sub>4</sub><sup>+</sup>-treated rats could be observed. (1) The initial rate of recovery (indicated by the dashed line) was significantly increased in NH<sub>4</sub><sup>+</sup>-treated animals by a factor of 2.4. Recovery rates were compared at identical pHi values. In normal rats the initial recovery rate was 0.24 ± 0.0309 pH units min<sup>-1</sup> (n = 10) as compared to 0.64 ± 0.09 pH units min<sup>-1</sup> (n = 11) in NH<sub>4</sub><sup>+</sup>-treated animals. (2) From Fig. 9 it is also apparent that the new resting pHi value after re-addition of Na<sup>+</sup> is significantly higher in NH<sub>4</sub><sup>+</sup>-treated animals. In NH<sub>4</sub><sup>+</sup>-treated animals the Na<sup>+</sup>-dependent increase to a new stable pHi value amounted to 0.38 ± 0.03 pH units (n = 11) as compared to 0.22 ± 0.02 pH units (n = 10) in untreated

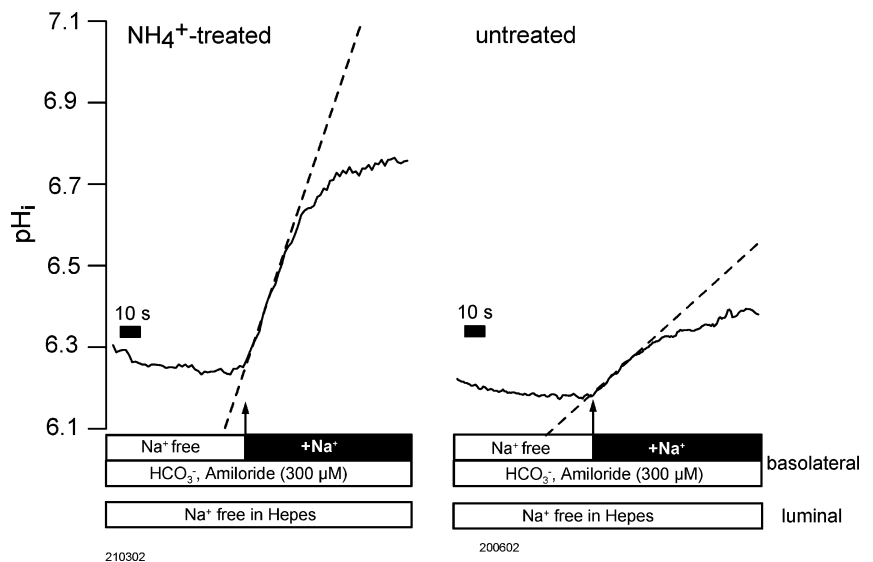
animals. Calculating initial J<sub>base</sub> after re-addition of Na<sup>+</sup> (see Methods) revealed 8.4 ± 0.9 pmol min<sup>-1</sup> mm<sup>-1</sup> in normal and 21.8 ± 3.2 pmol min<sup>-1</sup> mm<sup>-1</sup> in rats treated with NH<sub>4</sub><sup>+</sup> and thus a 2.6-fold increase of HCO<sub>3</sub><sup>-</sup> flux. Taken together these data indicate a strong functional up-regulation of Na<sup>+</sup>-dependent HCO<sub>3</sub><sup>-</sup> influx in NH<sub>4</sub><sup>+</sup>-treated animals.

**Cl<sup>-</sup> independence of Na<sup>+</sup>-dependent HCO<sub>3</sub><sup>-</sup> influx in normal and NH<sub>4</sub><sup>+</sup>-treated animals**

The family of Na<sup>+</sup>-dependent HCO<sub>3</sub><sup>-</sup> transporters also encompasses Cl<sup>-</sup>-dependent transporters (NDCBE: Na<sup>+</sup>-dependent Cl<sup>-</sup>-HCO<sub>3</sub><sup>-</sup> exchangers). We therefore repeated the experiments described in Fig. 9 in the absence of luminal and basolateral Cl<sup>-</sup>. The same protocol was used as described for the experiments shown in Figs 6 and 9. Two original traces are shown in Fig. 10 in normal and NH<sub>4</sub><sup>+</sup>-treated tubules. Cl<sup>-</sup> was removed bilaterally 17.8 ± 3.2 min (n = 5) before re-addition of basolateral Na<sup>+</sup>. Clearly it is seen that addition of Na<sup>+</sup> induces a rapid alkalinization and that this alkalinization is strongly up-regulated in NH<sub>4</sub><sup>+</sup>-treated rats. Table 3 summarizes all results. In chloride-free conditions a 3-fold up-regulation of Na<sup>+</sup>-dependent base influx was measured in NH<sub>4</sub><sup>+</sup>-treated rats. Also in these experiments the Na<sup>+</sup>-dependent increase to a new stable pHi value was significantly larger in NH<sub>4</sub><sup>+</sup>-treated rats (0.47 ± 0.04 pH units, n = 5) as compared to untreated animals (0.23 ± 0.05 pH units, n = 5). Table 3 shows that in both experimental series the up-regulation on Na<sup>+</sup>-dependent HCO<sub>3</sub><sup>-</sup> influx in NH<sub>4</sub><sup>+</sup>-treated animals was of similar magnitude. These

**Figure 9. Comparison of Na<sup>+</sup>-dependent re-alkalinization in normal and NH<sub>4</sub><sup>+</sup>-treated animals**

The protocol was as described in Fig. 4. Left panel: NH<sub>4</sub><sup>+</sup>-treated animals. Right panel: untreated animals. The dashed lines indicate the initial rate of re-alkalinization. In NH<sub>4</sub><sup>+</sup>-treated animals a significantly faster rate of re-alkalinization is obvious. In addition a significantly higher steady state pHi after Na<sup>+</sup>-dependent HCO<sub>3</sub><sup>-</sup> influx is reached in NH<sub>4</sub><sup>+</sup>-treated animals.



experiments clearly indicate that  $\text{Na}^+$ -dependent  $\text{HCO}_3^-$  influx occurs independently of  $\text{Cl}^-$  and thus argues for NBCn1 as the relevant transporter.

### DIDS-insensitivity of basolateral $\text{Na}^+$ -dependent $\text{HCO}_3^-$ influx

To further characterize  $\text{Na}^+$ -dependent  $\text{HCO}_3^-$  influx we subsequently investigated its possible DIDS sensitivity. The experiments were conducted with the same protocol as those described in Fig. 6 and performed using animals treated with  $\text{NH}_4^+$  in their drinking water for 1 week. An original experiment is shown in Fig. 11. Acid loading was again performed by removing luminal  $\text{Na}^+$ . Basolateral amiloride ( $300 \mu\text{M}$ ) was present during the entire relevant experimental period. In  $\text{CO}_2/\text{HCO}_3^-$ -containing buffer, rapid alkalinizations are visible whenever  $\text{Na}^+$  was re-added. These  $\text{Na}^+$ -dependent rapid alkalinizations represent  $\text{HCO}_3^-$  influx. Removal of  $\text{Na}^+$  resulted in a return to the acidic pre-control  $\text{pH}_i$  value of near 6.3. During the second addition of  $\text{Na}^+$ , DIDS ( $400 \mu\text{M}$ ) was present (including the indicated preincubation period of 60–90 s). As shown in Fig. 11 this had no effect on  $\text{Na}^+$ -dependent  $\text{HCO}_3^-$  influx. Similar results were observed in 10 experiments (pH recovery rate before DIDS:  $0.63 \pm 0.11$ , during DIDS  $0.68 \pm 0.16$  and after washout of DIDS  $0.67 \pm 0.17$  pH units  $\text{min}^{-1}$ ). These results indicate that basolateral  $\text{Na}^+$ -dependent  $\text{HCO}_3^-$  influx is not blocked by DIDS. DIDS-mediated inhibition of another  $\text{HCO}_3^-$  transporter located in the basolateral membrane of mTAL could, however, be shown. Medullary TAL segments also express a basolateral  $\text{Cl}^-$ - $\text{HCO}_3^-$  antiporter, which

is known to be DIDS inhibitable. Functional activity of the  $\text{Cl}^-$ - $\text{HCO}_3^-$  antiporter can be made visible by removing basolateral  $\text{Cl}^-$ . This is known to induce rapid, reversible alkalinizations (Sun, 1998). As shown in Fig. 12, alkalinization mediated by  $\text{Cl}^-$  removal was almost completely inhibited with  $400 \mu\text{M}$  DIDS ( $n = 3$ ). These experiments strengthen the results indicating that  $\text{Na}^+$ -dependent  $\text{HCO}_3^-$  influx in rat mTAL is not blocked by DIDS.

### Discussion

This study serves to increase our understanding of the recently identified electroneutral  $\text{Na}^+$ -dependent  $\text{HCO}_3^-$  transporter NBCn1 localized in rat inner stripe mTAL segments (Choi *et al.* 2000). A preceding immunolabelling study indicated the localization of NBCn1 in the basolateral membrane of mTAL segments (Vorum *et al.* 2000). Thus, the initial purpose was to identify  $\text{Na}^+$ -dependent  $\text{HCO}_3^-$  influx across the basolateral membrane of mTAL segments. This required the use of the isolated perfused kidney tubule technique to achieve sufficient control over the different luminal and basolateral acid–base transporters known in this segment. Our results identify  $\text{Na}^+$ -dependent  $\text{HCO}_3^-$  influx across the basolateral membrane of mTAL segments. We propose that this  $\text{HCO}_3^-$  influx is mediated via the NBCn1 protein. To investigate this further we studied  $\text{Na}^+$ -dependent  $\text{HCO}_3^-$  influx in normal and  $\text{NH}_4^+$ -treated animals. The addition of  $\text{NH}_4^+$  to the drinking water is a well-established method of producing a model of chronic metabolic acidosis which has previously been shown to induce a strong up-regulation of NBCn1 protein in mTAL (Kwon *et al.* 2002). This up-regulation is confirmed in this study. We hypothesized that protein up-regulation should be reflected in the up-regulation of  $\text{Na}^+$ -dependent  $\text{HCO}_3^-$  influx. Indeed, our experiments show a strong and significant up-regulation of  $\text{Na}^+$ -dependent  $\text{HCO}_3^-$  influx in rats treated with  $\text{NH}_4^+$ . Therefore, the close correlation between up-regulation of protein and function strengthens the proposal that NBCn1 mediates  $\text{Na}^+$ -dependent  $\text{HCO}_3^-$  influx in rat mTAL. Importantly, a near to identical  $\text{Na}^+$ -dependent  $\text{HCO}_3^-$  influx in control rats was observed in the absence of  $\text{Cl}^-$ . Likewise in  $\text{NH}_4^+$ -treated rats  $\text{Cl}^-$  depletion left the strong up-regulation of  $\text{Na}^+$ -dependent  $\text{HCO}_3^-$  influx unchanged (Fig. 10 and Table 3). This strongly indicates that  $\text{Na}^+$ -dependent  $\text{HCO}_3^-$  influx in rat mTAL does not occur via the closely related  $\text{Na}^+$ -dependent  $\text{Cl}^-$ - $\text{HCO}_3^-$  exchangers.

DIDS is a widely used inhibitor of anion and  $\text{HCO}_3^-$  transport (Cabantchik & Greger, 1992). Our study presents

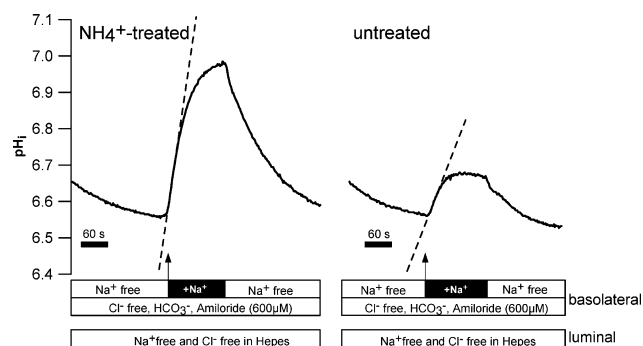


**Figure 10. Comparison of  $\text{Na}^+$ -dependent re-alkalinization in normal and  $\text{NH}_4^+$ -treated animals under  $\text{Cl}^-$ -free conditions**  
The protocol was as described in Fig. 4. Left panel:  $\text{NH}_4^+$ -treated animals. Right panel: untreated animals. The dashed lines indicate the initial rate of re-alkalinization. Also after removal of bilateral  $\text{Cl}^-$  in  $\text{NH}_4^+$ -treated animals a significantly faster rate of re-alkalinization is obvious. In addition a significantly higher steady state  $\text{pH}_i$  after  $\text{Na}^+$ -dependent  $\text{HCO}_3^-$  influx is reached in  $\text{NH}_4^+$ -treated animals.

**Table 3. Summary of pHi recovery rate and base flux data in normal and NH<sub>4</sub><sup>+</sup>-treated rats**

		Untreated	NH <sub>4</sub> <sup>+</sup> treated
With chloride (n = 11)	pHi recovery (pH units min <sup>-1</sup> )	0.24 ± 0.03	0.64 ± 0.09
	Base flux (pmol min <sup>-1</sup> mm <sup>-1</sup> )	8.4 ± 0.9	21.8 ± 3.2
Without chloride (n = 5)	pHi recovery (pH units min <sup>-1</sup> )	0.28 ± 0.04	0.72 ± 0.25
	Base flux (pmol min <sup>-1</sup> mm <sup>-1</sup> )	8.7 ± 1.36	26.1 ± 9.3

evidence that the basolateral Na<sup>+</sup>-dependent HCO<sub>3</sub><sup>-</sup> influx is not blocked by DIDS. This is in close agreement with the initial cloning paper showing a very low DIDS sensitivity (Choi *et al.* 2000) Some DIDS sensitivity was, however, observed in a preceding study in which the entire kidney slice was used to measure pHi *in situ* in mTAL segments (Kwon *et al.* 2002). Currently we do not believe that our recently shown DIDS sensitivity of Na<sup>+</sup>-dependent recovery from acid load in whole kidney slices reflects NBCn1 function alone (Kwon *et al.* 2002). The observed DIDS insensitivity supports the interpretation that Na<sup>+</sup>-dependent HCO<sub>3</sub><sup>-</sup> influx is mediated via NBCn1.

Noteworthy is a recent study which investigated a number of basolateral acid–base transporters in isolated perfused rat mTAL segments. The authors reported Na<sup>+</sup>-dependent HCO<sub>3</sub><sup>-</sup> influx over the basolateral membrane and similarly found no effects of DIDS (Bourgeois *et al.* 2002). In addition they performed their experiments in Cl<sup>-</sup>-free medium, indicating that Na<sup>+</sup>-dependent HCO<sub>3</sub><sup>-</sup> transport occurs independently of Cl<sup>-</sup>. Thus this study is in close agreement with our results presented here.

### Is NBCn1 the only basolateral Na<sup>+</sup>-dependent HCO<sub>3</sub><sup>-</sup> importer in mTAL?

A recent publication indicates that in addition to NBCn1 yet another variant of Na<sup>+</sup>-dependent HCO<sub>3</sub><sup>-</sup> transporters, namely NBC4, could be present in rat mTAL segments as based on mRNA data (Xu *et al.* 2002). However, our RT-PCR results did not detect NBC4 message in isolated mTAL tubules. Since the rat genome has become available in 2003 we found that the primers used by Xu *et al.* to identify NBC4 in rat kidney do not recognize any relevant sequence of the rat NBC4 gene (SLC4A5). Furthermore a BLAST search revealed that the forward primer (ATGGTTGACCGATCCTTG) used by Xu *et al.* matches mouse NBC3. The reverse primer (GCTGGCTCTTAATAATGATGGC) identified 30 different sequences of diverse origin and not related to NBC sequences. We currently do not believe that rat

mTAL express NBC4 and think that the above-mentioned study is faulty. In addition our RT-PCR did not show the expression of other known members of the Na<sup>+</sup>-coupled HCO<sub>3</sub><sup>-</sup> transporters NCBE (Wang *et al.* 2000; Choi *et al.* 2002) and NDCBE (Grichtchenko *et al.* 2000). Immunolabelling studies furthermore strengthened the findings that electrogenic NBCe1 is only expressed in the proximal tubules of the renal cortex and that no NH<sub>4</sub><sup>+</sup>-induced expression occurs in mTAL segments. Our screen also included the functionally still uncharacterized BTR1 protein which, based on a homology analysis, was suggested to be a HCO<sub>3</sub><sup>-</sup> transporter (Parker *et al.* 2001). As shown we could identify BTR1 message in isolated rat mTAL tubule; however, its significance is currently obscure.

As mentioned above the rat NBCn1 protein is a close homologue of the human NBC3 protein (Pushkin *et al.* 1999). Recently an NBC3 knock-out mouse was generated with the somewhat surprising phenotype of developing blindness and deafness (Bok *et al.* 2003). An apparent renal phenotype was not observed. This mouse will enable us to definitively investigate if in mTAL the NBCn1/NBC3 protein is the only Na<sup>+</sup>-dependent HCO<sub>3</sub><sup>-</sup> transporter. Nonetheless our compiled data strongly suggest that NBCn1 is probably the only protein involved in basolateral Na<sup>+</sup>-dependent HCO<sub>3</sub><sup>-</sup> uptake and is strongly up-regulated during metabolic acidosis. Our results however, do not explicitly rule out that other unforeseen candidates may contribute to this function.

Functionally basolateral Na<sup>+</sup>-H<sup>+</sup> exchange (NHE1, NHE4) and Na<sup>+</sup>-dependent HCO<sub>3</sub><sup>-</sup> uptake could serve the same purpose, namely to extrude acid equivalents from the cytosol. Na<sup>+</sup>-dependent recovery rates in the presence and absence of CO<sub>2</sub>/HCO<sub>3</sub><sup>-</sup>-containing buffer allow the quantification of the contribution of the two mechanisms involved. NBC-mediated recovery in normal rats was 0.24 ± 0.03 pH units min<sup>-1</sup>. In comparison NHE-mediated recovery from acid amounted to 0.26 ± 0.05 pH units min<sup>-1</sup>. Interestingly, we found no up-regulation of NHE-mediated recovery from acid load in NH<sub>4</sub><sup>+</sup>-treated rats. Confirmatory results were presented on the levels of the

protein and mRNA for NHE1, where no up-regulation was observed in metabolic acidosis (Laghmani *et al.* 2001). In addition, our own immunolabelling results confirm that NHE1 is not up-regulated in  $\text{NH}_4^+$ -treated animals (authors' unpublished observations).

An integrated functional role for NBCn1 in mTAL may become apparent when we consider the major functions of mTAL. As summarized in the Introduction mTAL is critically involved in  $\text{NaCl}$ ,  $\text{Mg}^{2+}$ ,  $\text{Ca}^{2+}$ ,  $\text{HCO}_3^-$  absorption and  $\text{NH}_4^+$  excretion. Considering the absorptive functions of mTAL, no direct involvement may intuitively be reasonable as basolateral  $\text{Na}^+$  influx may appear counterproductive and  $\text{HCO}_3^-$  absorption requires a basolateral  $\text{HCO}_3^-$  exit step and not the contrary. However, the function of  $\text{NH}_4^+$  excretion may indeed profit from a basolateral  $\text{HCO}_3^-$  importing mechanism. The functional concept is schematically

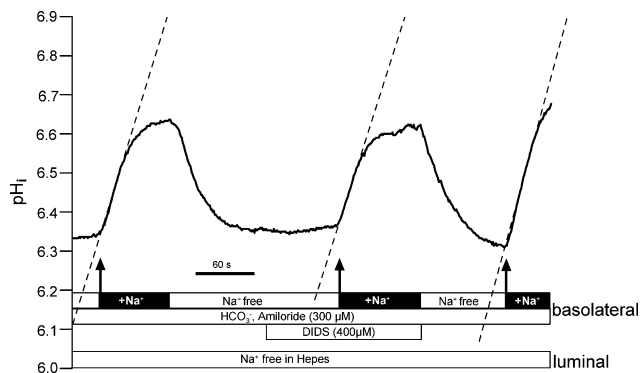


**Figure 11.** No effect of DIDS on  $\text{Na}^+$ -dependent re-alkalinization in an  $\text{NH}_4^+$ -treated animal

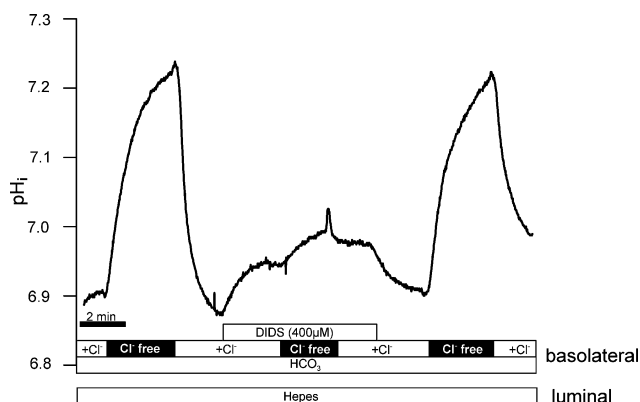


**Figure 12.** Effect of DIDS on alkalization induced by removal of extracellular  $\text{Cl}^-$

Note that DIDS had a prompt and rapid alkalizing effect on resting  $\text{pH}_i$ . The subsequent  $\text{Cl}^-$ -removal-induced alkalization was almost completely inhibited with  $400 \mu\text{M}$  DIDS. The DIDS inhibition was reversible.

shown in Fig. 13 and has already been mentioned in some detail in the Introduction. Metabolic acidosis is associated with increased proximal tubular formation of  $\text{NH}_4^+$  and subsequently its handling along the tubulus (Curthoys & Gstraunthaler, 2001). It is suggested that basolateral NBCn1 serves to maintain medullary transcellular  $\text{NH}_4^+$  shuttling by maintaining a favourable mTAL  $\text{pH}_i$ . Luminal entry of  $\text{NH}_4^+$  via the NKCC2 transporter and the ROMK channel is well established and results in a large and continuous acid load of the mTAL cell (Good, 1994). The nature of this significant  $\text{NH}_4^+$ -induced acid load is complex, including more than the uptake of a proton via  $\text{NH}_4^+$  (Good, 1994). An acidic  $\text{pH}_i$  of the mTAL cell will reduce the diffusible fraction of  $\text{NH}_3$  ( $\text{pK}_b$ , 9.3). On the contrary a more alkaline  $\text{pH}_i$  should significantly increase the free diffusible  $\text{NH}_3$  and thus will allow basolateral  $\text{NH}_3$  exit and further trapping of  $\text{NH}_3/\text{NH}_4^+$  in the acidic collecting duct fluid. It remains to be measured more directly, however, whether functional NBCn1 is significantly required for unrestrained  $\text{NH}_4^+$  excretion.

In summary this study strongly suggests that basolateral  $\text{Na}^+$ -dependent  $\text{HCO}_3^-$  uptake occurs via NBCn1. This  $\text{Na}^+$ -dependent  $\text{HCO}_3^-$  influx occurs independently of  $\text{Cl}^-$ . In isolated perfused mTAL segments NBCn1 was found to be DIDS insensitive. Chronic metabolic acidosis induced a strong up-regulation of NBCn1 protein and function. We suggest that NBCn1-mediated  $\text{HCO}_3^-$  uptake is an important event in transcellular transport of  $\text{NH}_4^+$ .

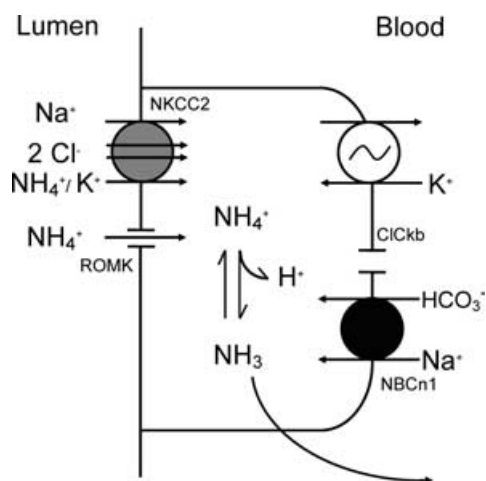


**Figure 13.** Schematic cell model of transcellular  $\text{NH}_4^+$  transport in medullary thick ascending limb

NBCn1 is suggested to be important for buffering the acid load imposed on the cell by uptake of luminal  $\text{NH}_4^+$  via the NKCC2 transporter and ROMK channels.

## References

- Bok D, Galbraith G, Lopez I, Woodruff M, Nusinowitz S, BeltrandelRio H, Huang W, Zhao S, Geske R, Montgomery C, Van Sligtenhorst I, Friddle C, Platt K, Sparks MJ, Pushkin A, Abuladze N, Ishiyama A, Dukkipati R, Liu W & Kurtz I (2003). Blindness and auditory impairment caused by loss of the sodium bicarbonate cotransporter NBC3. *Nat Genet* **34**, 313–319.
- Bourgeois S, Masse S, Paillard M & Houillier P (2002). Basolateral membrane  $\text{Cl}^-$ ,  $\text{Na}^+$ , and  $\text{K}^+$ -coupled base transport mechanisms in rat MTALH. *Am J Physiol Renal Physiol* **282**, F655–F668.
- Cabantchik ZI & Greger R (1992). Chemical probes for anion transporters of mammalian cell membranes. *Am J Physiol* **262**, C803–C827.
- Choi I, Aalkjaer C, Boulpaep EL & Boron WF (2000). An electroneutral sodium/bicarbonate cotransporter NBCn1 and associated sodium channel. *Nature* **405**, 571–575.
- Choi I, Rojas JD, Kobayashi C & Boron W (2002). Functional characterization of 'NCBE', a  $\text{Na}/\text{HCO}_3$  cotransporter. *FASEB J* **16**, A796.
- Curthoys NP & Gstraunthaler G (2001). Mechanism of increased renal gene expression during metabolic acidosis. *Am J Physiol Renal Physiol* **281**, F381–F390.
- Good DW (1985). Sodium-dependent bicarbonate absorption by cortical thick ascending limb of rat kidney. *Am J Physiol* **248**, F821–F829.
- Good DW (1994). Ammonium transport by the thick ascending limb of Henle's loop. *Annu Rev Physiol* **56**, 623–647.
- Good DW, Knepper MA & Burg MB (1984). Ammonia and bicarbonate transport by thick ascending limb of rat kidney. *Am J Physiol* **247**, F35–F44.
- Good DW & Watts BA III (1996). Functional roles of apical membrane  $\text{Na}^+/\text{H}^+$  exchange in rat medullary thick ascending limb. *Am J Physiol* **270**, F691–F699.
- Greger R (1985). Ion transport mechanisms in thick ascending limb of Henle's loop of mammalian nephron. *Physiol Rev* **65**, 760–797.
- Greger R & Hampel W (1981). A modified system for in vitro perfusion of isolated renal tubules. *Pflugers Arch* **389**, 175–176.
- Grichtchenko II, Romero MF & Boron WF (2000). Extracellular  $\text{HCO}_3^-$  dependence of electrogenic  $\text{Na}/\text{HCO}_3$  cotransporters cloned from salamander and rat kidney. *J Gen Physiol* **115**, 533–546.
- Kwon TH, Fulton C, Wang W, Kurtz I, Frokiaer J, Aalkjaer C & Nielsen S (2002). Chronic metabolic acidosis upregulates rat kidney  $\text{Na}-\text{HCO}$  cotransporters NBCn1 and NBC3 but not NBC1. *Am J Physiol Renal Physiol* **282**, F341–F351.
- Laghmani K, Richer C, Borensztein P, Paillard M & Froissart M (2001). Expression of rat thick limb  $\text{Na}/\text{H}$  exchangers in potassium depletion and chronic metabolic acidosis. *Kidney Int* **60**, 1386–1396.
- Maunsbach AB, Vorum H, Kwon TH, Nielsen S, Simonsen B, Choi I, Schmitt BM, Boron WF & Aalkjaer C (2000). Immunoelectron microscopic localization of the electrogenic  $\text{Na}/\text{HCO}_3$  cotransporter in rat and amblyoma kidney. *J Am Soc Nephrol* **11**, 2179–2189.
- Parker MD, Ourmozdi EP & Tanner MJ (2001). Human BTR1, a new bicarbonate transporter superfamily member and human AE4 from kidney. *Biochem Biophys Res Commun* **282**, 1103–1109.
- Pushkin A, Abuladze N, Lee I, Newman D, Hwang J & Kurtz I (1999). Cloning, tissue distribution, genomic organization, and functional characterization of NBC3, a new member of the sodium bicarbonate cotransporter family. *J Biol Chem* **274**, 16569–16575.
- Roos A & Boron WF (1981). Intracellular pH. *Physiol Rev* **61**, 296–434.
- Sun A (1998). Expression of  $\text{Cl}^-/\text{HCO}_3^-$  exchanger in the basolateral membrane of mouse medullary thick ascending limb. *Am J Physiol* **274**, F358–F364.
- Sun AM, Kikeri D & Hebert SC (1992). Vasopressin regulates apical and basolateral  $\text{Na}^+ - \text{H}^+$  antiporters in mouse medullary thick ascending limbs. *Am J Physiol* **262**, F241–F247.
- Thomas JA, Buchsbaum RN, Zimniak A & Racker E (1979). Intracellular pH measurements in Ehrlich ascites tumor cells utilizing spectroscopic probes generated in situ. *Biochemistry* **18**, 2210–2218.
- Vorum H, Kwon TH, Fulton C, Simonsen B, Choi I, Boron W, Maunsbach AB, Nielsen S & Aalkjaer C (2000). Immunolocalization of electroneutral  $\text{Na}-\text{HCO}_3^-$  cotransporter in rat kidney. *Am J Physiol Renal Physiol* **279**, F901–F909.
- Wang CZ, Yano H, Nagashima K & Seino S (2000). The  $\text{Na}^+$ -driven  $\text{Cl}^-/\text{HCO}_3^-$  exchanger – Cloning, tissue distribution, and functional characterization. *J Biol Chem* **275**, 35486–35490.
- Watts BA III & Good DW (1994). Apical membrane  $\text{Na}^+/\text{H}^+$  exchange in rat medullary thick ascending limb. pH-dependence and inhibition by hyperosmolality. *J Biol Chem* **269**, 20250–20255.
- Weiner ID & Hamm LL (1989). Use of fluorescent dye BCECF to measure intracellular pH in cortical collecting tubule. *Am J Physiol* **256**, F957–F964.
- Wright PA, Burg MB & Knepper MA (1990). Microdissection of kidney tubule segments. *Meth Enzymol* **191**, 226–231.
- Xu J, Wang Z, Barone S, Petrovic M, Amlal H, Conforti L, Petrovic S & Soleimani M (2002). The expression of  $\text{Na}^+ - \text{HCO}_3^-$  cotransporter NBC4 in rat kidney and characterization of a novel NBC4 variant. *Am J Physiol Renal Physiol* **284**, F41–F50.

**Acknowledgements**

We thank Susie Mogensen, Edith Bjørn Møller, Kirsten Skaarup, Ann-Charlotte Andersen, Ida Maria Jalk and Inger Merete Poulsen for their expert technical assistance. Support for

this study was provided by the Danish Medical Research Council and the Water and Salt Research Center at the University of Aarhus which is established and supported by the Danish National Research Foundation (Danmarks Grundforskningsfond).